Chapter 4. The biology and chemistry of discodermolide

4.1 Introduction

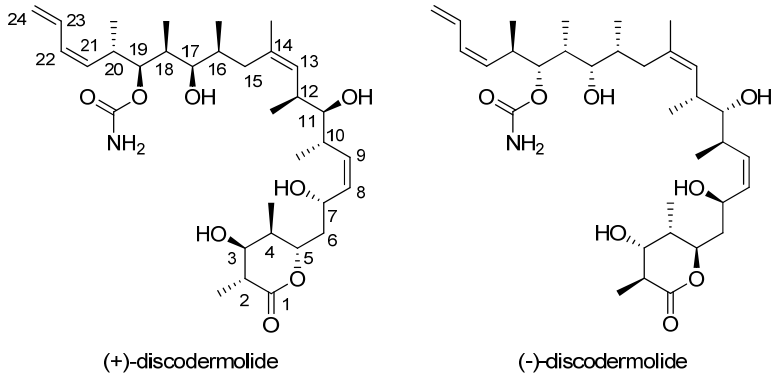

Figure 4.1 Structures of (+)-discodermolide and (-)-discodermolide

In 1990, Sarath P. Gunasekera and co-workers isolated a new polyketide natural product named discodermolide,[1] from a Caribean marine sponge, *Discodermia dissolute*, which was collected at Lucay, Grand Bahama Island at a depth of 33 m. This place had previously been recognized as a source of a number of structurally interesting and potent biological agents such as calyculins A-D[2,3] and discodermins A-D.[4] Discodermolide is a crystalline solid that degrades when being dried under vacuum at room temperature, but is relatively stable in MeOH or EtOAc. Its structure was elucidated by Gunasekera's group through several spectroscopic techniques including NMR spectroscopy, IR, UV and MS, and was then verified by X-ray crystallographic analysis.[1] The absolute

configuration was defined by Schreiber and co-workers in 1993 through total synthesis.[5] As shown in Figure 4.1, its structure comprises a linear polyketide backbone with 13 chirality centers, 3 *Z*-double bonds, a carbamate at C-9, a terminal *cis*-diene and a δ-lactone. To minimize the strains and steric interactions, a hairpin-shaped conformation is generally believed to be preferred by discodermolide in both the solid state and solution.[6,7] (-)-Discodermolide, the enantiomer of discodermolide, is not naturally available and was first synthesized in 1993 by Schreiber's group for the purpose of determining the absolute stereochemistry and finding the cellular target of (+)-discodermolide.[5,8] Similar to paclitaxel, both discodermolide and its enantiomer arrest the cell cycle at a stage after entering mitosis by inducing the polymerization of tubulins and stabilizing microtubules, ultimately leading to cell death.[9,10,11] Importantly, discodermolide shows greater efficiency in stabilization of microtubules than paclitaxel, a compound that has played an important role in cancer chemotherapy during the past two decades. Of particular interest is that discodermolide displays potent activity against multi-drug-resistant cancer cell lines including paclitaxel-resistant cancer cell lines,[12] and that the combination of paclitaxel and discodermolide exhibits synergistic drug effects in cultured cell lines.[13]

4.2 Bioactivity

Discodermolide was initially isolated as a potent immunosuppressive and antifungal substance.[14,15] But its bioactivity was then proved not to be limited only to the immune system.[8,14,15] Remarkably, it displayed impressive and outstanding cytotoxicity. In 1994, Schreiber's group reported that discodermolide inhibited incorporation of tritiated thymidine into DNA with IC_{50} values of 7 nM and 35 nM for discodermolide and its enantiomer, respectively, in several cell lines.[8] In further investigation, discodermolide was found to be toxic in human and murine cell lines with IC_{50} values of 3-80 nM,[11] which led to a large number of further explorations to its mechanisms of action.

4.2.1 Cell cycle arrest

The studies on the distribution of a population of cells in the cell cycle through measurement of the DNA content in cells by flow cytometry found that cells treated with discodermolide were arrested at the G_2/M phase, while (-)-discodermolide blocked the cell cycle at S phase, both of which eventually led to the cell death. In comparison, the population of untreated cells (vehicle control) remained mainly in the G_1 phase. Interestingly, the arresting phases in the cell cycle were totally different for the two enantiomers, indicating that they acted through distinct mechanisms.

To further define the arresting mechanism, investigations on the effect of discodermolide on cyclin B expression were performed.[10,11] In various eukaryotic cells, cyclin B associated with and activated the kinase cdc2, and the expression of cyclin B resulted in activating M-phase-promoting factor (MPF), which drove the cell cycle into mitosis.[18-20] More importantly, at the anaphase of mitosis, degradation of cyclin B that subsequently deactivated MPF took place, which allowed the separation of sister chromatids, chromosome decondensation, cytokinesis, and nuclear envelope reformation, indicating that the degradation of cyclin B was necessary for cell mitosis.[21-23] These studies revealed that discodermolide treatment displayed no effects on the expression of cyclin B at the beginning of cell cycle. However, the following degradation of cyclin B at anaphase of mitosis was clearly delayed by about 6-12 hours in the presence of discodermolide. During this prolonged period, the cells had the same morphology as mitotic cells, and finally re-adhered instead of undergoing mitosis as usual. The re-adhered cells were mostly micronucleated and larger in size than the control cells.

4.2.2 Tubulin polymerization and microtubule stabilization

Nearly all anti-mitotic reagents, including colchicines, colcemid and paclitaxel, were proved to interact with microtubules,[24-27] which promoted researchers into further explorations on the effect of discodermolide on microtubules for better understanding of

its mechanism of action.

4.2.2.1 Effects of discodermolide on intracellular microtubules

The *in vivo* target of discodermolide was reported to be the intact microtubules by Schreiber's group in 1996.[10] It was then found that discodermolide treated cells contained dense and discontinuous bundles of microtubules, instead of the continuous network of microtubules in control cells. So similarly to paclitaxel, discodermolide caused a major rearrangement of cellular microtubules. In comparison with untreated cells, MCF-7 cells treated with discodermolide at concentrations as high as 10 nM contained filamentous and bundled microtubules retracted and concentrated around the nucleus, while treatment with 10 nM of paclitaxel had little effect on the overall appearance of the cellular microtubule network.[11] Even treated with 10 μM of paclitaxel, the bundled microtubules were less extensive than occurred with 1 μM of discodermolide.[11] Therefore, discodermolide induced microbubule bundle formation more potently than paclitaxel.

Furthermore, it was found that the higher the concentration of discodermolide, the more prominent and elongated the formed bundles became.[11] Indirect immunofluorescence studies revealed that microtubule bundles appeared more rapidly after discodermolide treatment than after paclitaxel treatment, although ultimately both of them indistinguishably led to complete reorganization of microtubules into bundles with multiple regions of nucleation.[12] Meanwhile, similarly to paclitaxel, discodermolide

stabilized microtubules upon cold treatment *in vivo*, whereas the microtubule bundles in control Swiss 3T3 cells completely disappeared upon incubation at 4 ˚C for 16 hours, but discodermolide clearly stabilized microtubules better than paclitaxel.[10] In addition, in treated A549 cells, bundle formations observed with discodermolide were distinctly different from those noticed with paclitaxel. The microtubule bundles were formed at the periphery of the cells in the presence of discodermolide, in contrast to cells treated by paclitaxel where the bundles appeared throughout the cell.[28] Further investigations found that similarly to paclitaxel, discodermolide altered the microtubule dynamic parameters and so stabilized intracellular microtubules, which was proved to be related to its ability to inhibit proliferation and block mitosis.[29]

4.2.2.2 Effects of discodermolide on tubulin assembly and microtubule stability[8,10-12,29]

In the absence of microtubule-associated proteins (MAPs), which are necessary for tubulin polymerization *in vitro* in general, 10 μM of discodermolide alone rapidly induced polymerization of tubulin.[10] By comparing the effect of 10 μM of discodermolide with 10 μM of paclitaxel in inducing polymerization of tubulin *in vitro*, it was proved that more vigorous assembly occurred with discodermolide than with paclitaxel. In the presence of GTP and MAPs, tubulin was rapidly polymerized immediately after addition

of 10 μM discodermolide at 0 ˚C, while paclitaxel treatment did not induce polymerization under the same conditions and significant assembly did not happen until the temperature reached 10 ˚C. In comparison, polymerization in the absence of discodermolide or paclitaxel occurred only at temperatures above 37 ˚C.

Further explorations on the combined effects of low temperature and Ca^{2+} on paclitaxel- and discodermolide-induced tubulin polymers in the present of GTP and MAPs found that 0.6 mM $CaCl_2$ caused greater than 90% disassembly of the polymer at 37 ˚C in the reaction with neither paclitaxel nor discodermolide, and higher concentrations of $CaCl_2$ caused more rapid and more extensive depolymerization. But $CaCl_2$ with a concentration as high as 5 mM caused no significant disassembly of the polymer induced by either paclitaxel or discodermolide at 37 ˚C. When the reaction temperature was decreased to 0 ˚C, paclitaxel-induced polymer underwent relatively rapid disassembly. On the contrary, the discodermolide-induced polymer treated with $CaCl_2$ was completely stable at 0 ˚C.

It was also found that at 0 ˚C tubulin polymerization without GTP was slower than that with GTP. In addition, in the absence of GTP, the concentration of $CaCl_2$ made little difference in the destabilizing effects of $CaCl_2$. In the absence of MAPs, polymerization by discodermolide at 0 ˚C was extremely slow. When the temperature was raised to 37 ˚C, the discodermolide-induced assembly became vigorous. With GTP and no MAPs, only

discodermolide-induced polymer was stable at 0 ˚C. Paclitaxel completely lost its tubulin polymerization activity in the absence of both GTP and MAPs, whereas discodermolide remained active at 37 ˚C. Furthermore, the critical concentrations of tubulin for assembly with paclitaxel and dicodermolide were reported,[12] as listed in Table 4.1. The literature critical concentration data, combined with the findings above, confirmed that the potency of discodermolide in inducing microtubule assembly reactions was significantly greater than that of paclitaxel.

Table 4.1 Critical concentrations of tubulin for assembly with paclitaxel and discodermolide

Drug	Critical concentration of tubulin (μM)			
	MAPs and GTP	MAPs only	GTP only	No MAPs or GTP
paclitaxel	0.24±0.3	1.7±0.4	4.3±0.4	22±1
discodermolide	0.41±0.4	0.93±0.2	0.88±0.4	3.0±0.3

Studies on the binding of tritiated discodermolide to microtubules showed that discodermolide bound to microtubules with a binding stoichiometry of one discodermolide per tubulin dimer. Additionally, it was proved by drug binding competition assay that discodermolide was an excellent inhibitor of the binding of ^{3}H-paclitaxel to the preformed microtubules. In comparison, paclitaxel only weakly inhibited the binding of ^{3}H-discodermolide to polymer even at higher concentrations. These results suggested that discodermolide and paclitaxel bound to mutually exclusive

(the same or overlapping) sites on microtubules and that discodermolide displayed better binding affinity to microtubules than paclitaxel.

Electron microscopy (EM) revealed that discodermolide produced large numbers of much shorter microtubules (0.53-0.59 μm) than those formed in the presence of paclitaxel (0.70-1.69 μm) which was still relatively shorter than those in a control sample (3.26±1.61 μm),[11,28] indicating that discodermolide had a major effect on microtubule nucleation. In addition, GTP and MAPs were both observed to affect discodermolide-induced microtubule morphology.[11,12] GTP caused more sheet formation instead of microtubules formation than MAPs. In the absence of both MAPs and GTP, a greater proportion of discodermolide-induced polymer had microtubule morphology than in absence of MAPs only. Addition of $CaCl_2$ did not affect discodermolide-induced polymer morphology, neither did lowering temperature. Therefore, the discodermolide-induced polymer was relatively more stable to both $CaCl_2$ and cold-induced disassembly.

4.2.2.3 Distinct binding and cellular properties between (+)-discodermolide and (-)-discodermolide[8]

In ^{3}H-thymidine incorporation assays, (+)-discodermolide (IC_{50}= 7 nM) was observed

to be ten times more potent than its enantiomer. In addition, as described above, (+)-discodermolide arrested the cell cycle at the G2/M phase, while (-)-discodermolide blocked cell cycle at the S phase. Of particular interest was that (-)-discodermolide was not a competitive inhibitor for binding of tritiated (+)-discodermolide to microtubules, which suggested that these two enantiomers arrested the cell cycle at different stages by interacting with distinct cellular targets.

4.2.2.4 Synergistic suppression

As mentioned above, the competitive binding of discodermolide to paclitaxel-induced microtubules suggested that they shared a common binding site on microtubules. Surprisingly, recent studies discovered that these two drugs could synergize to inhibit proliferation of A549 human lung cancer cells when used simultaneously.[29] They also synergistically inhibited overall microtubule dynamic properties in living cells, blocked the cell cycle at G_2/M, and promoted apoptosis, more effectively than individually.[30] Several mechanisms could probably explain the synergism between discodermolide and paclitaxel.[30] One possibility was that the two drugs altered the subtle conformation of the microtubules where they were bound, which resulted in increased stability of the microtubule lattice. It was also very possible that paclitaxel might enhance positively the binding of discodermolide to microtubules or enhance the factor that could help

discodermolide bind to microtubules. Their synergy might also result from differential binding of the two drugs to the various tubulin isotypes, which might lead to an altered overall microtubule architecture and synergy. Importantly, these findings provided a novel and interesting strategy for combining low doses of drugs in cancer chemotherapy.

4.2.2.5 Activity against multidrug-resistant (MDR) cancer cell lines

Of the most promising features, discodermolide displayed much greater activity against MDR cancer cell lines than paclitaxel.[12] Although the parental carcinoma lines generally were more sensitive to paclitaxel than discodermolide, the corresponding paclitaxel-resistant cell lines as a consequence of genetic alterations of a β–tubulin gene showed much more sensitivity to discodermolide. This suggested that the affinity of the altered tubulin for paclitaxel decreased significantly, while the affinity for discodermolide probably just changed a little or did not change.

4.3 Structure-activity relationships (SAR)

The structure of discodermolide comprises a complex linear polypropionate backbone, including 13 chirality centers, 3 *Z*-double bonds at C8-C9, C13-C14 and C21-C22, a carbamate at C-9, a terminal *cis*-diene at C21-C24 and a δ-lactone. For better

understanding of its mechanism of binding to microtubules, the elucidation of its structure-activity relationships is necessary. As mentioned above, to minimize the strains and steric interactions, a hairpin-shaped conformation is generally believed to be preferred by discodermolide in both the solid state and solution.[6] Several other important SAR findings had been reported on discodermolide during the past decade (Figure 4.2).[9,28,29,31-35]

The C1 position can be thiophenylated without affecting the bioactivity.[9] The elimination of both the C2 methyl and the C3 hydroxyl groups dramatically increased the cytotoxicity of discodermolide by 10 times.[36] Acetylation at the C3 hydroxyl group has little effect on the cytotoxicity of discodermolide, and the absence of the C3 hydroxyl group surprisingly enhances cytotoxicity,[13,36] so it is not essential for the bioactivity. Silylation at C3 dramatically decreases the cytotoxicity,[35] so presumably there is a spatial constant at this position. Discodermolide can thus tolerate modification on the lactone ring to different extents depending on how the structure is modified.[37] Surprisingly, replacement of the δ-lactone with certain 5-membered rings enhanced the cytotoxicity, whereas significant loss of cytotoxicity was observed when replacing the δ-lactone with various aryl groups[29] or acyl groups.[38] It was also reported that replacement of the lactone ring by an aromatic ring could possibly preserve the cytotoxicity of discodermolide if it maintained the appropriate orientation.[37]

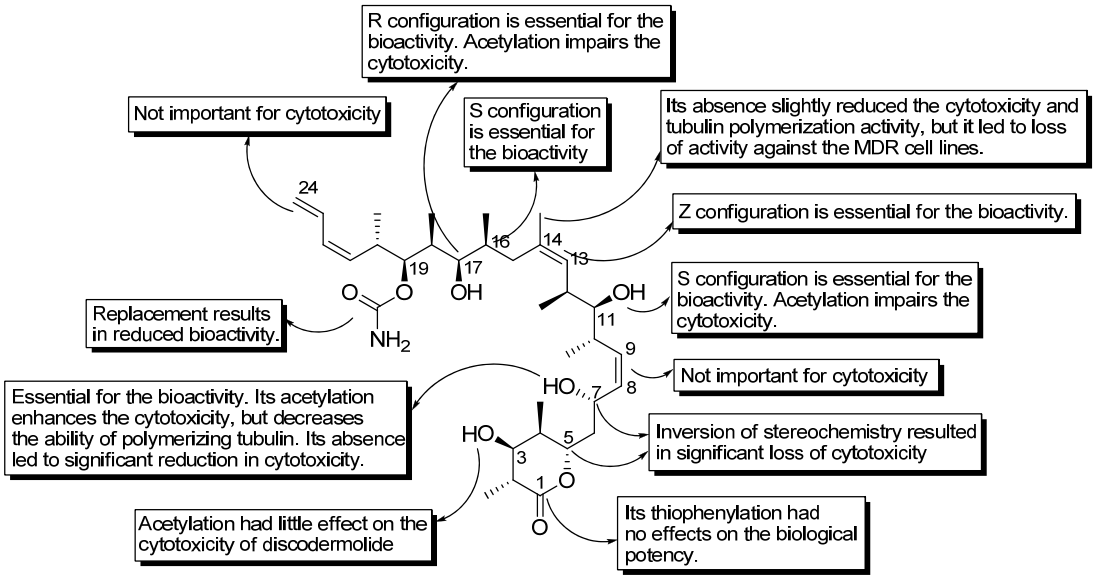

Figure 4.2 Structure-activity relationships for discodermolide

Inversion of stereochemistry at C7 and C5 led to significant loss of activity.[39] In addition, acetylation of the C7 hydroxyl group enhanced the cytotoxicity of the molecule against A549 cells. Interestingly, discodermolide was found to be more effective in polymerizing purified tubulin than the compound with the C7 hydroxyl group acetylated, indicating that either acetylated discodermolide at C7 is more cell-membrane permeable, or that acetylation at the C7 hydroxyl group induced additional cytotoxic qualities not present in the original discodermolide molecule. The absence of the hydroxyl group at C7 resulted in an apparent reduction in bioactivity, indicating the importance of the C7 hydroxyl group for cytotoxicity of discodermolide.

In contrast to acetylation at C3 or C7, acetylation of the hydroxyl groups at the C11 and C17 positions severely reduced the cytotoxicity of the molecule. Further studies

showed that chemical modifications of the central region (C11, C17) in the discodermolide molecule served to impair its biological activities, which indicated that these hydroxyl moieties played significant roles in the overall antimitotic activity of discodermolide. Furthermore, epimerization of the C17 hydroxyl group made the final molecule inactive, and inversion of stereochemistry at C11 greatly reduced the bioactivity of the overall molecule. Together, these results indicated the essential roles of the hydroxyl groups at C7, C11 and C17 in maintaining the favorable stereochemistry of the pharmacophore, possibly through a hydrogen bonding interaction with the neighboring carbamate group.

Other SAR investigations revealed that both the C8-C9 *Z*-double bond and the terminal conjugated diene system were not contributing significantly to the cytotoxicity of discodermolide, whereas the C13-C14 *Z*-double bond, which was believed to partly control the folding of the discodermolide molecule to an optimum conformation in order to fit into the binding site, was crucial for the antimitotic activity, and the hydrogenation of this double bond resulted in complete loss of the bioactivity. The absence of the C14 methyl group slightly reduced the cytotoxicity and tubulin polymerization activity, but led to loss of activity against the NCI/ADR multidrug-resistant cell line. The replacement of the C13-C14 double bond by cyclopropane retained nanomolar cytoxicity against the drug-sensitive cell line but greatly reduced activities against the multidrug-resistant cell

line.

Additionally, the absence of the C16 methyl group had no effect on the bioactivity. On the contrary, inversion of the absolute configuration at C16 led to reduced cytotoxicity, indicating that C16 stereochemistry was essential for biological activity of discodermolide. The introduction of an acetoxy group at C19 in place of the carbamate was detrimental to the antimitotic activity of discodermolide. Modifications of the C19 carbamate maintained potent cytotoxicity in drug-sensitive cell lines, but led to the loss of cytotoxicity in multidrug-resistant cell lines. Importantly, the hairpin folding conformation bringing the δ-lactone end and the C19 side chain in close proximity was found to be essential for the biological activity of discodermolide.

4.4 Total Synthesis

Marine sources of discodermolide only provided minimal quantities of material (7 mg from 434 g frozen sponge).[40] Therefore, currently the only practical solution of this issue is total chemical synthesis. Several partial synthesis and total syntheses have been reported since 1993.[41-53,69] The retrosynthetic analysis of discodermolide for every synthetic approach is shown in Figure 4.3, and five well-known total synthetic routes are reviewed and discussed below.

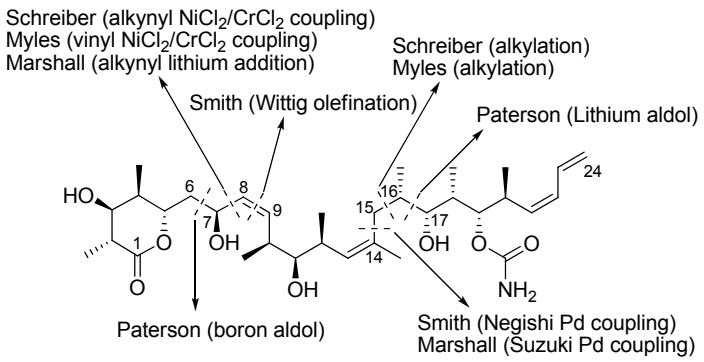

Figure 4.3 Retrosynthesis of discodermolide

4.4.1 The Schreiber Synthesis

Schreiber's group reported the first total synthesis of (-)-discodermolide in 1993,[5] before they developed a novel total synthetic route for discodermolide in 1996.[9] The retrosynthesis of discodermolide by Schreiber's group is shown in Scheme 4.1.

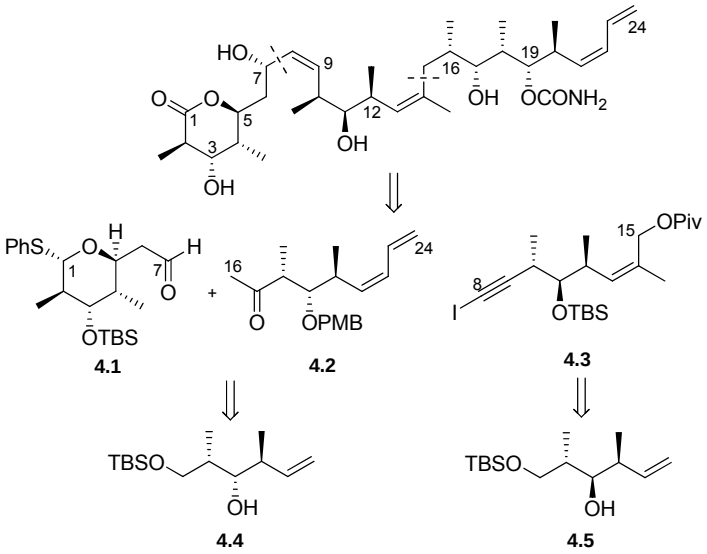

Scheme 4.1 Retrosynthesis of Schreiber's approach

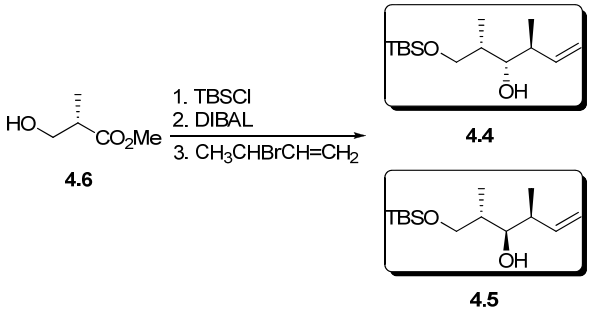

Scheme 4.2 Synthesis of fragment **4.4** and **4.5**

This synthetic approach began with a common commercial compound **4.6** as shown in Scheme 4.2. The addition of (*E*)- and (*Z*)-crotylboronate to **4.6** gave two stereospecific precursors **4.4** and **4.5**, respectively.[33]

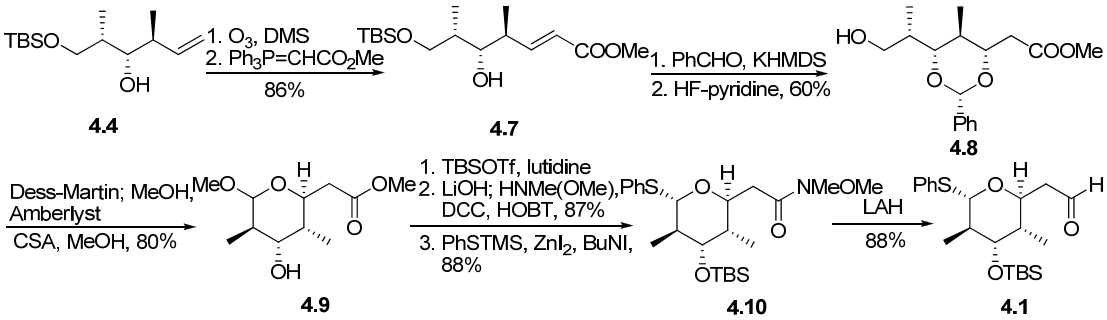

Scheme 4.3 Synthesis of fragment **4.1**

The common precursor **4.4** was then converted to ester **4.7** via ozonolysis and Wittig olefination, which was then converted to alcohol **4.8**. **4.8** was subject to Dess-Martin oxidation and cyclization reaction to give **4.9**, which was converted to fragment **4.1** in four steps with good yield. To synthesize fragment **4.2**, the common precursor **4.4** was protected as its PMB ether and then converted to vinyl iodide **4.11** via ozonolysis and

Wittig olefination. Then the terminal diene was installed to give **4.12** by a palladium-catalyzed coupling with vinylzinc bromide. Deprotection of the TBS group with trifluoroacetic acid, Dess-Martin oxidation and subsequent Grignard addition of methylmagnesium bromide provided fragment **4.2** in good yield.

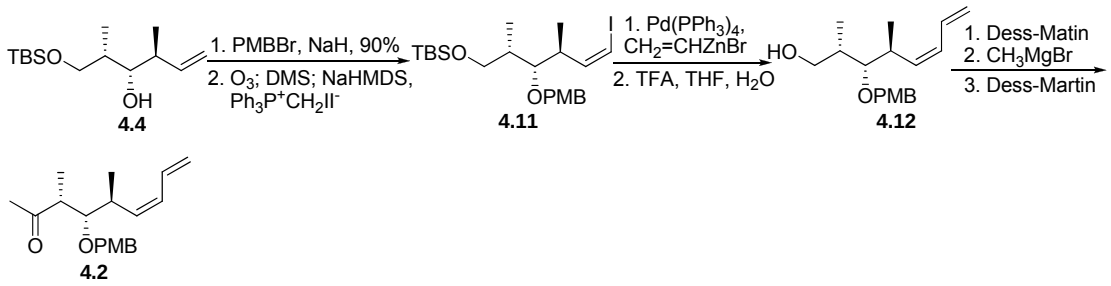

Scheme 4.4 Synthesis of fragment **4.2**

The other precursor **4.5** was transformed into *Z*-trisubstituted oldfin **4.13** by the method of Still and Gennari,[54] which was then converted to fragment **4.3** in four steps.

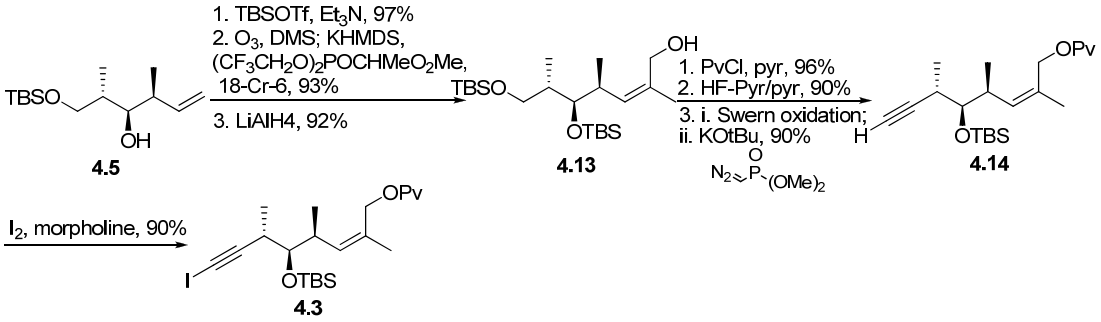

Scheme 4.5 Synthesis of fragment **4.3**

The Nozaki-Kishi coupling of thioacetal **4.1** and iodoacetylene **4.3** yielded **4.15** as the major epimer in a 2:1 mixture of diastereomers,[55] which was subsequently converted to **4.16** by hydrogenation, TBS protection and the DIBAL deprotection of the pivaloate.

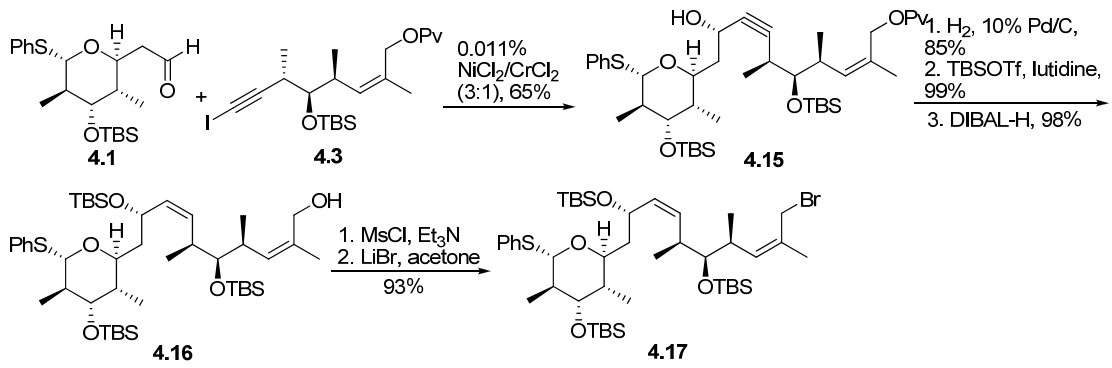

Scheme 4.6 Synthesis of fragment **4.17**

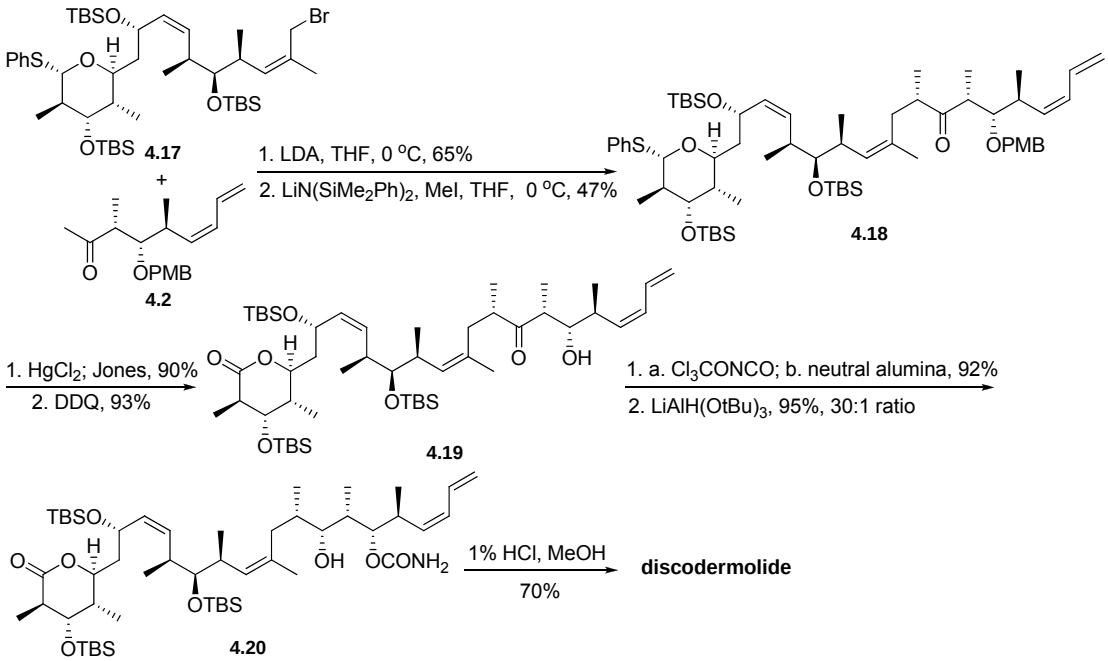

Scheme 4.7 Synthesis of discodermoldie

After the conversion of alcohol **4.16** to **4.17**, the alkylation of methyl ketone **4.2** with bromide **4.17** followed by methylation provided an access to compound **4.18**.[41,50] Subsequent conversion of **4.18** to **4.19** followed by selective reduction with LiAlH(*t*-BuO)$_3$ and acidic deprotection of the protecting groups completed the synthesis

of discodermolide in 36 steps with 4.3% overall yield. This synthesis provided a good solution to the supply problem of discodermolide for further biological studies. Although several steps somehow gave poor selectivity and yields, for example, the Nozaki-Kishi coupling of compound **4.1** and **4.3** only gave poor stereoselectivity, in favor of the desired configuration, their strategy did open an access for the following synthetic studies.

4.4.2 The Smith Synthesis

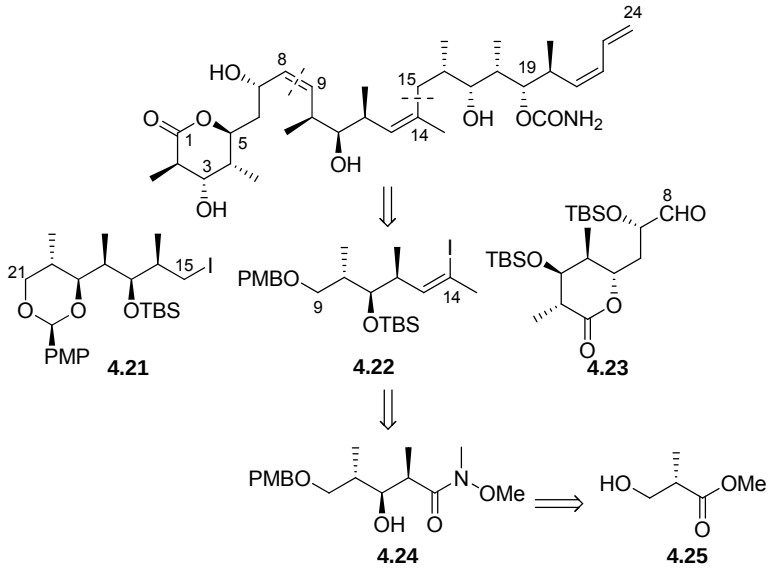

Scheme 4.8 Retrosynthesis of Smith's appoach

In 1995, after the first total synthesis of (-)-discodermolide by Schreiber's group, Smith's group developed a different strategy to synthesize (-)-discodermolide (first-generation synthesis).[63] Then they reported the improved second- and

third-generation syntheses of discodermolide in 1999 and 2003, respectively.[64-66] As shown below, a triply convergent approach was utilized in Smith's synthesis, dissecting (+)-discodermolide at C8-C9 and C14-C15 to generate subunits **4.21**, **4.22** and **4.23**, each of which was prepared from a common precursor **4.24**, which was considered the great appeal of the Smith's synthesis (Scheme 4.8).

It was noteworthy that the reaction sequence from **4.25** to **4.24** through Evan's aldol chemistry only involved one chromatographic separation step, which brought much convenience in practice (Scheme 4.9).

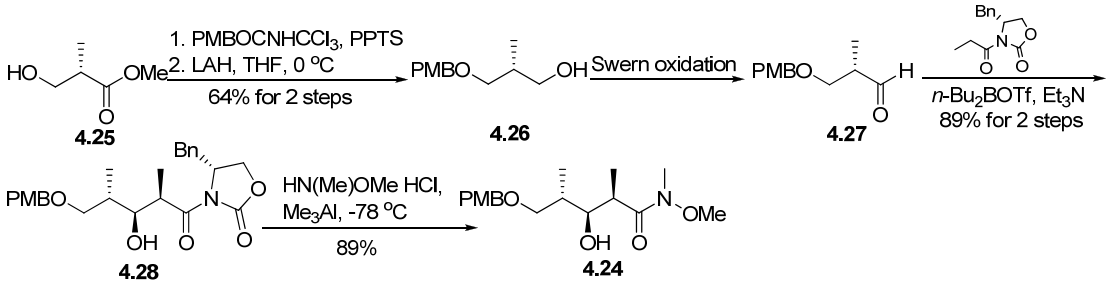

Scheme 4.9 Synthesis of the common precursor **4.24**

Three fragments **4.21**, **4.22** and **4.23** were obtained through the reactions starting from the common precursor **4.24** upon optimization of the chemistry developed in their first-generation synthesis (Scheme 4.10).[63]

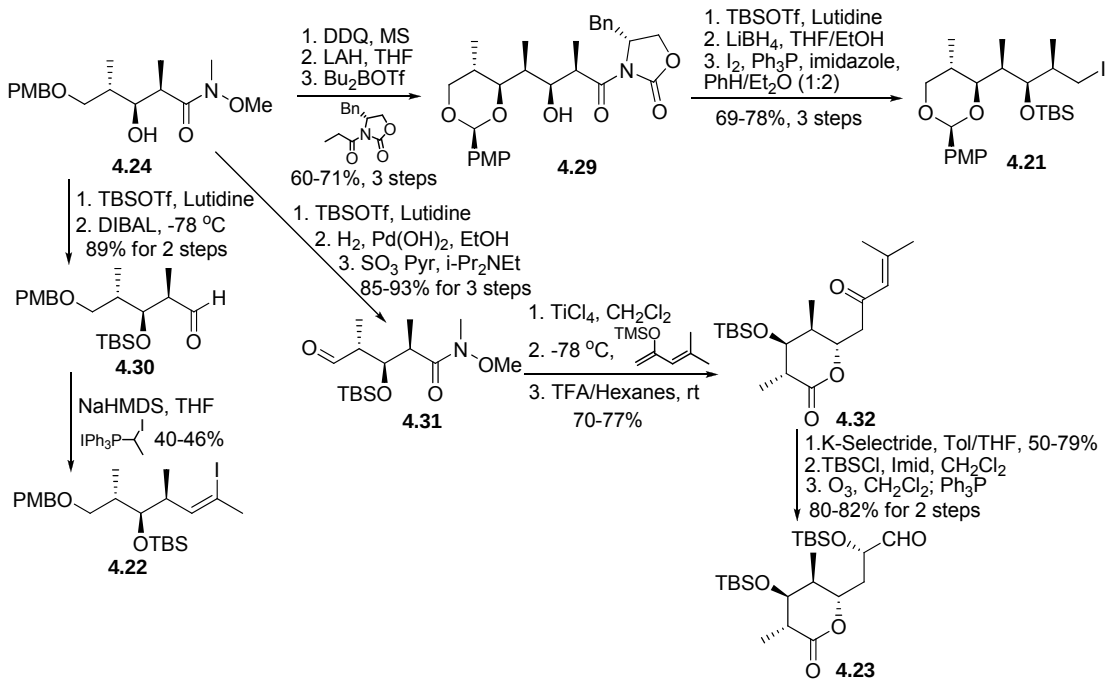

Scheme 4.10 Synthesis of fragments **4.21-4.23**

The revised palladium-catalyzed cross-coupling (Negishi coupling) of **4.21** and **4.22** provided **4.33** in a 73% yield based on starting purity of **4.22**.[67] The compound **4.33** was subsequently transformed to Wittig salt **4.36** followed by Wittig coupling with **4.23** to afford **4.37** in good yield with excellent *Z/E* selectivity (15-24:1). After removal of the protecting groups and installation of the carbamate at C19 via the Kocovsky protocol,[68] the discodermolide synthesis was completed in a yield of 6% (Scheme 4.11).

In 2003, they reported a practical improvement of this discodermolide synthesis, in which ultrahigh pressure was not required to access the Wittig salt used for constructing the C8-C9 disubstituted olefin, compared to relatively higher pressure required in second-generation synthesis.[65] In comparison with the other syntheses, this synthesis

showed higher efficiency, proceeded in higher yield, and was amenable to gram-scale production of discodermolide. Additionally, the notable features also included triple convergency, with each of the three subunits derived from the same precursor **4.24**, a modified Negishi coupling, efficient synthesis of phosphonium salt **4.36**, and a chemoselective Wittig coupling reaction.

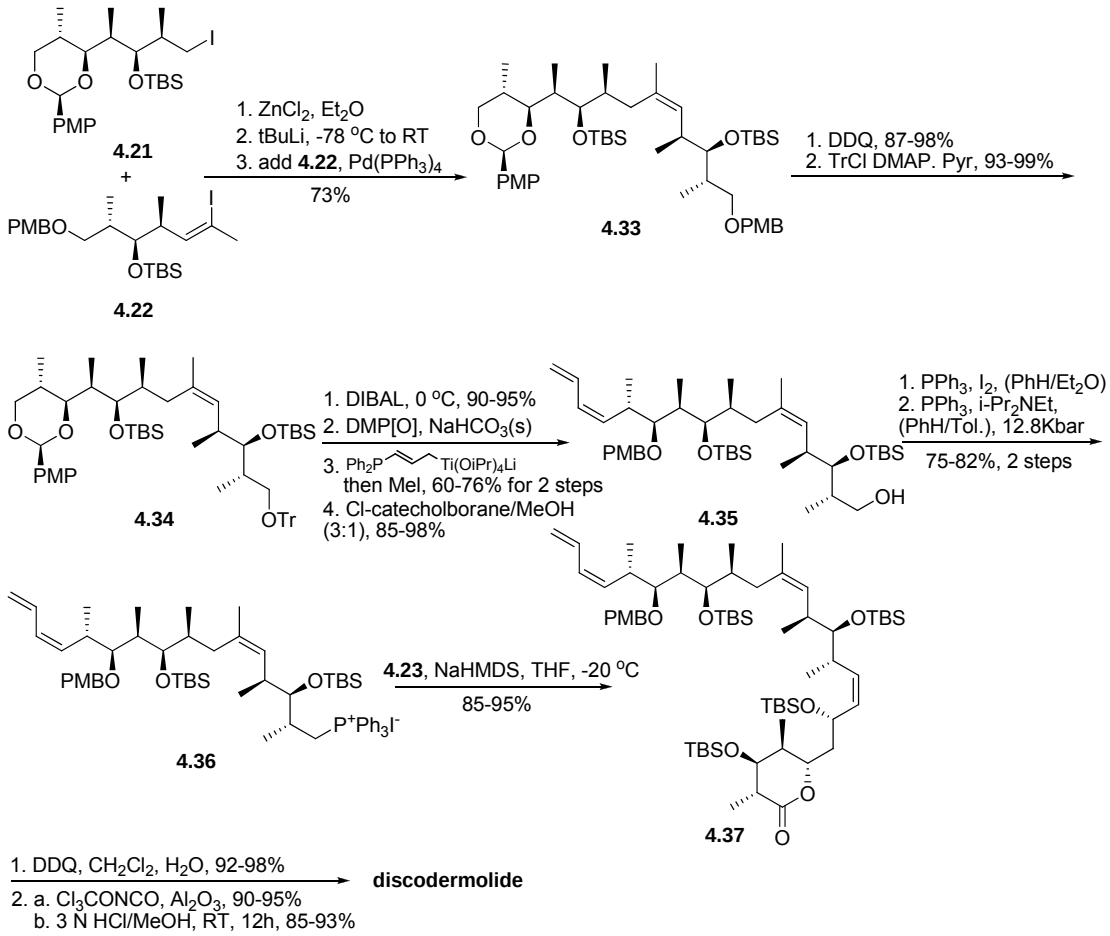

Scheme 4.11 Synthesis of discodermolide

4.4.3 The Myles Synthesis[52,56]

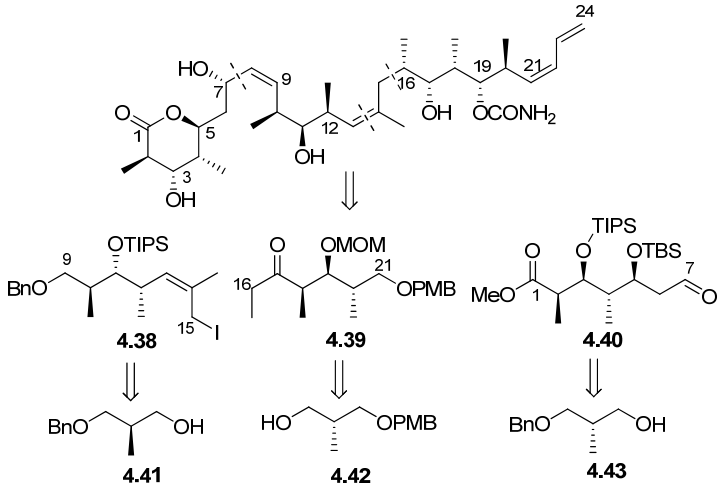

Scheme 4.12 Retrosynthesis of Myles's appoach

In 1997, Myles's group reported a total synthesis of (-)-discodermolide using chelation-controlled alkylation reaction as the key coupling.[52] Recently they reported another total synthesis of discodermolide, which adopted a similar strategy disconnecting the C7-C8 and C15-C16 bonds to give three key subunits (the retrosynthesis as shown in Scheme 4.12.[56]

The synthesis began with benzyl ether **4.41**, which was prepared from commercially available compounds.[71] The benzyl ether was oxidized to aldehyde **4.44** via Swern oxidation, and the following Lewis acid-catalyzed cyclocondensation reaction provided pyrone **4.45**. The following Luche reduction converted **4.45** to intermediate **4.46**, which underwent reduction to open the lactols ring to give diol **4.47**. Facile protecting group

manipulations then furnished allylic alcohol **4.48** in 85% yield, which was converted to allyl iodide **4.38** in 96% yield (Scheme 4.13).

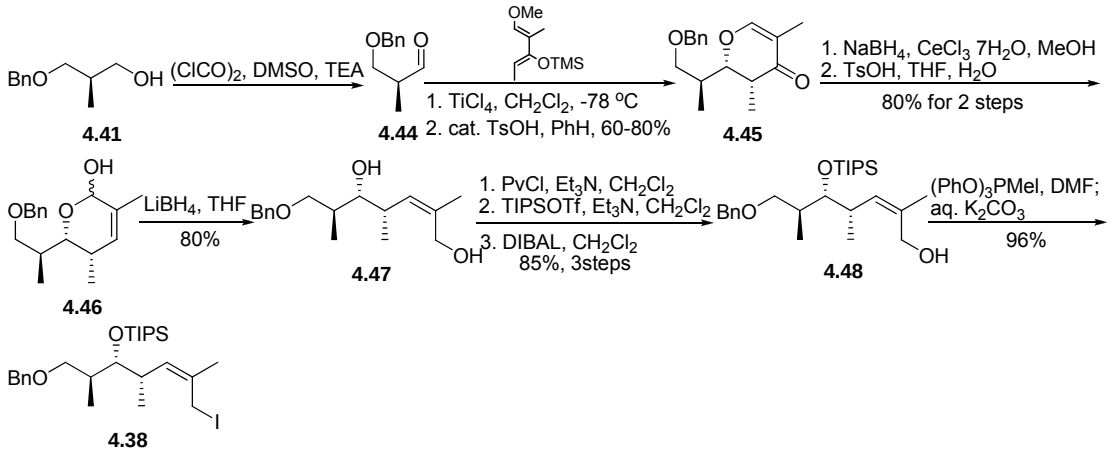

Scheme 4.13 Synthesis of fragment **4.38**

The synthesis of the subunit **4.39** began with PMB ether **4.42**, which was converted to **4.49** via Swern oxidation and Evan's aldol reaction in 88% yield. Then **4.49** was treated with trimethyl aluminum and *N*,*O*-dimethylhydroxylamine to produce the Weinreb amide, which was finally converted to ethyl ketone **4.39** via MOM protection and Grignard reaction (Scheme 4.14).

To prepare subunit **4.40**, benzyl ether **4.43** was oxidized and allylated to give alcohol **4.50**. TBS protection and Bn deprotection provided TBS ether **4.51**, which was subsequently oxidized and treated under Evan's aldol conditions to furnish alcohol **4.52**. This material was treated with lithium hydroperoxide to cleave the chiral auxiliary and the resulting acid was converted to methyl ester **4.53** by treatment with

(trimethylsilyl)diazomethane in 79% yield over four steps. Finally, TIPS protection followed by ozonolysis provided aldehyde **4.40** (Scheme 4.15).

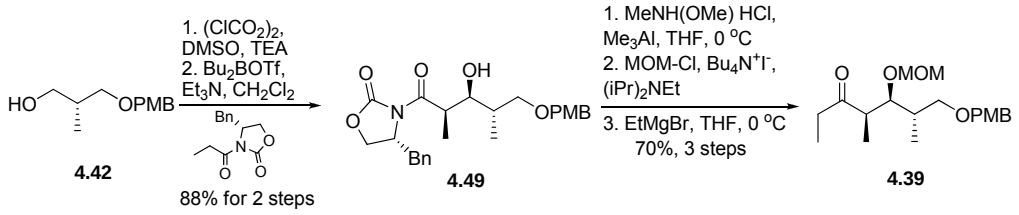

Scheme 4.14 Synthesis of fragment **4.39**

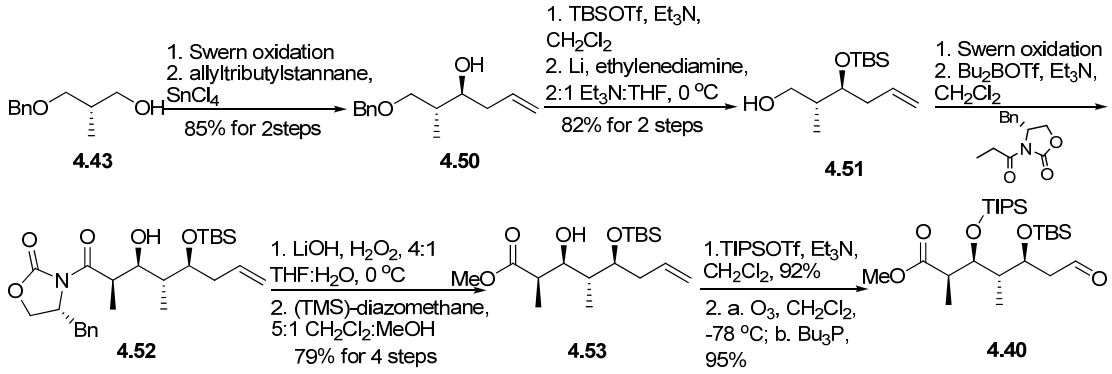

Scheme 4.15 Synthesis of fragment **4.40**

Allyl iodide **4.38** and ethyl ketone **4.39** were treated with LiHMDS and TMEDA to give alkene **4.54** in 70% yield (Scheme 4.16). After the conversion of ketone **4.54** to alcohol **4.55**, protection of the resulting alcohol as its TIPS ether, followed by chemoselective deprotection of the benzyl ether using H_2 and Raney Ni provided primary alcohol **4.56** in 71% yield over two steps. Alcohol **4.56** was subsequently oxidized to aldehyde, which underwent Wittig reaction to give vinyl iodide **4.57** in 90% yield. The following PMB deprotection and oxidation furnished aldehyde **4.58**, which was then

converted to diene **4.59** by treatment with (trimethylsilyl)allylboronate reagent and potassium hydride with the desired geometry in 80% yield over two steps. The deprotection of MOM ether followed by the installation of carbamate moiety at C19 position afforded vinyl iodide **4.60**.

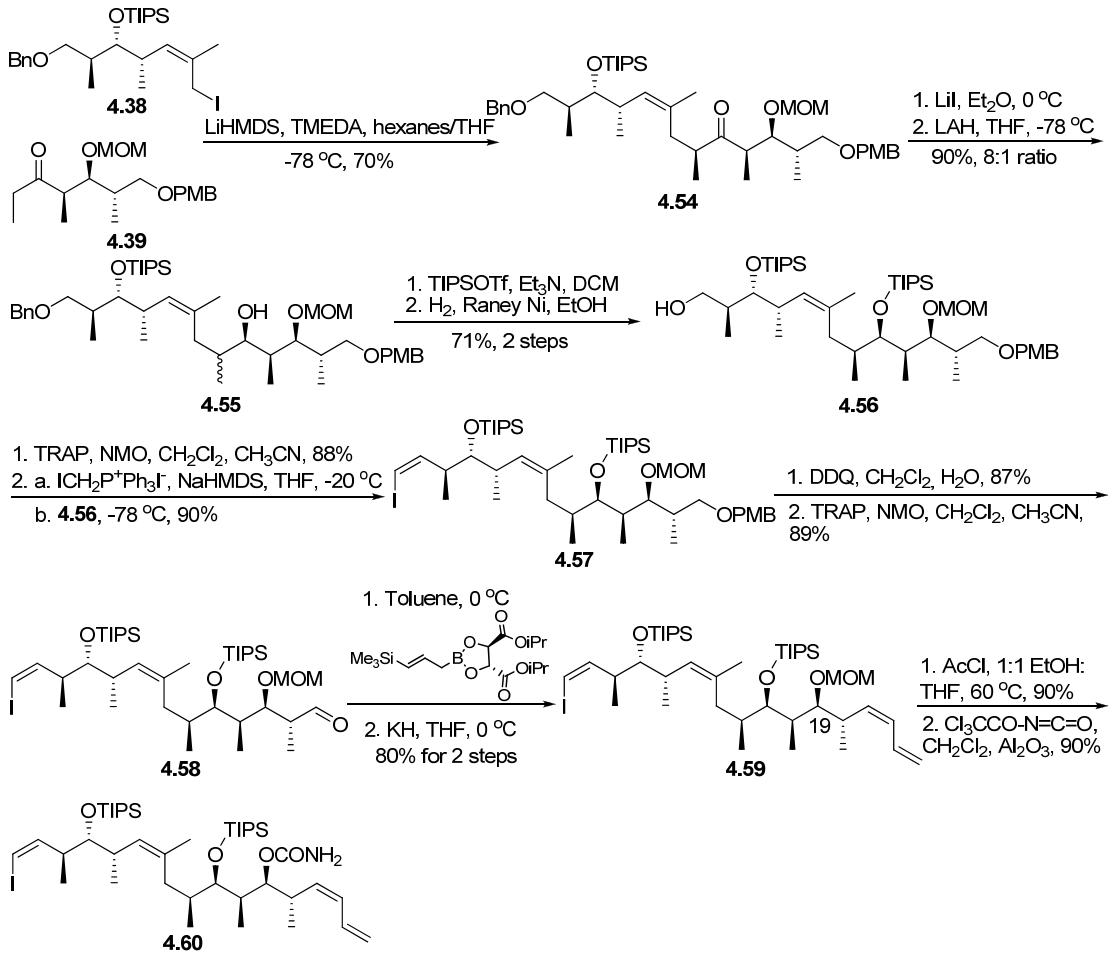

Scheme 4.16 Synthesis of intermediate **4.60**

The coupling between vinyl iodide **4.60** and aldehyde **4.40** was accomplished by treatment with 1% $NiCl_2/CrCl_2$ and Kishi's chiral bispyridinyl ligand in THF in 42%

yield. The cyclization and global deprotection of sily protecting groups finally provided discodermolide in 52% yield over two steps. This synthesis proceeded in a highly convergent manner; the longest linear sequence for synthesizing discodermolide was 22 steps from aldehyde **4.44** in an overall yield of 1.5%. The synthesis of separate fragments and the coupling reactions of these fragments were readily amenable to large scale. The convergent strategy also allowed for the facile preparation of analogues of discodermolide (Scheme 4.17).

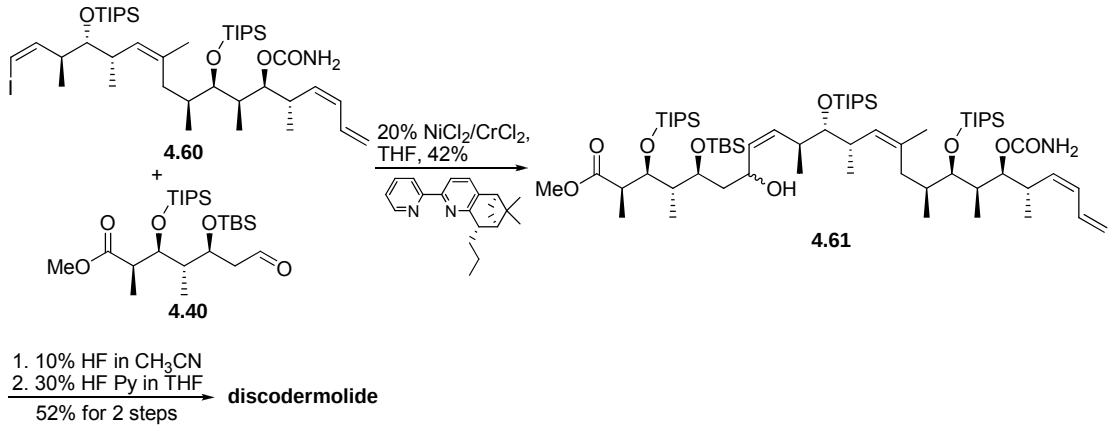

Scheme 4.17 Synthesis of discodermolide

4.4.4 The Marshall Synthesis[58]

In 1998, Marshall and co-workers developed a new synthetic route for discodermolide by using the strategy as shown above. The linear structure of discodermolide was disconnected at the C7-C8 and C14-C15 bonds to give three subunits

4.62, **4.63** and **4.64**, which were derived from starting material aldehyde **4.65** and **4.66** (Scheme 4.18).

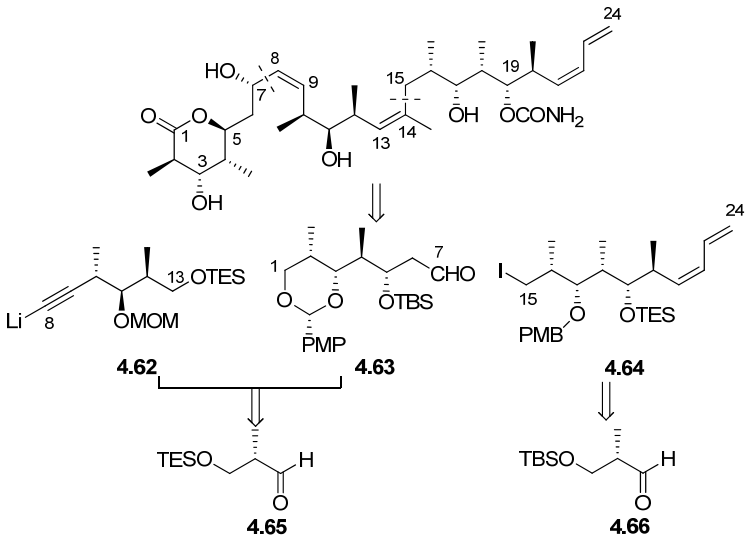

Scheme 4.18 Marshall's retrosynthetic appoach

The Marshall synthesis started from chiral alkynyl lithium **4.62** which were afforded from aldehyde **4.65** (Scheme 4.19). On the other hand, alkyne **4.67**, which was one of the intermediates in the synthesis of **4.64**, was converted to **4.63** via acetal **4.69** (Scheme 4.20).

To synthesize subunit **4.64**, the precursor **4.66** was treated with allenylstannane and trifluoroborane to provide alkyne **4.71**, which was converted to diene **4.72** in eleven steps in 39% yield (Scheme 4.21). The acetal **4.72** was subsequently treated with DIBAL-H followed by iodination to give iodide **4.64**.

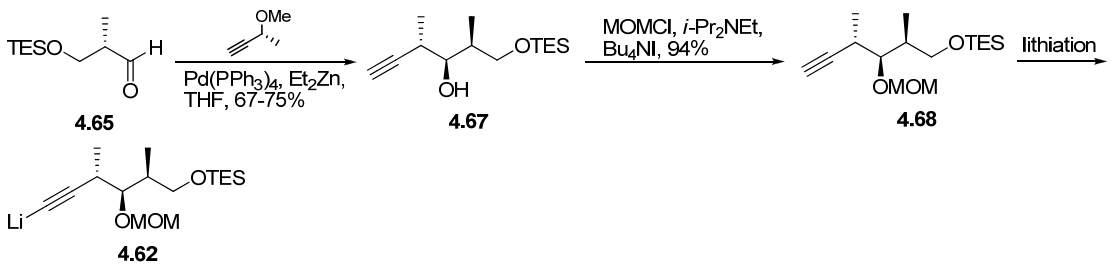

Scheme 4.19 Synthesis of fragment **4.62**

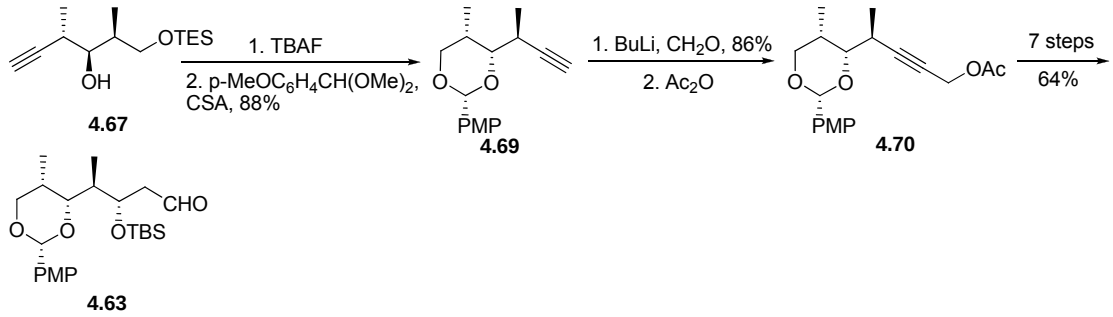

Scheme 4.20 Synthesis of Fragment **4.63**

The coupling of **4.62** and **4.63** was accomplished by treatment with lithium bromide in THF. The resulting alkyne **4.73** was hydrogenated, protected as MOM ether and TBS deprotected to give alcohol **4.74**, which was subject to Dess-Martin oxidation and Wittig coupling reaction to afford vinyl iodide **4.75** in 40% yield (Scheme 4.22). Iodide **4.64** was subsequently coupled with vinyl iodide **4.75** via Suzuki coupling reaction to furnish acetal **4.76**, which was converted to discodermolide via methyl ester **4.77** (Scheme 4.23).

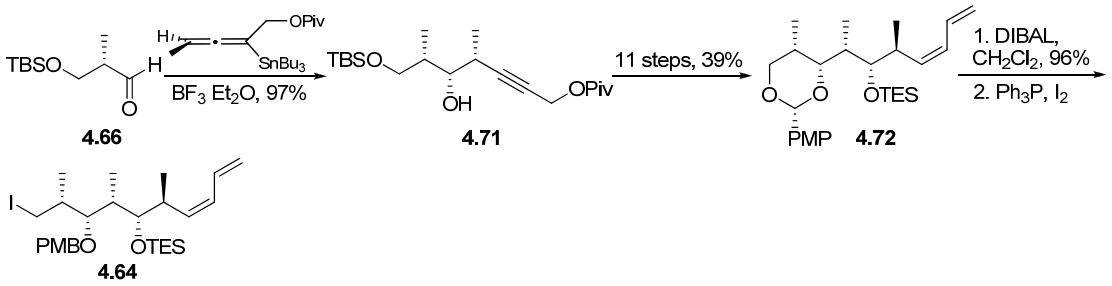

Scheme 4.21 Synthesis of Fragment **4.64**

The overall yield of the Marshall synthesis was about 1.2%. In the synthesis scheme, it is noteworthy that Suzuki coupling was utilized as the key coupling reaction to establish the skeleton of discodermolide. Meanwhile, the Marshall synthesis illustrated the potential of chiral allenyl metal reagents in the synthesis of polypropionate natural products.

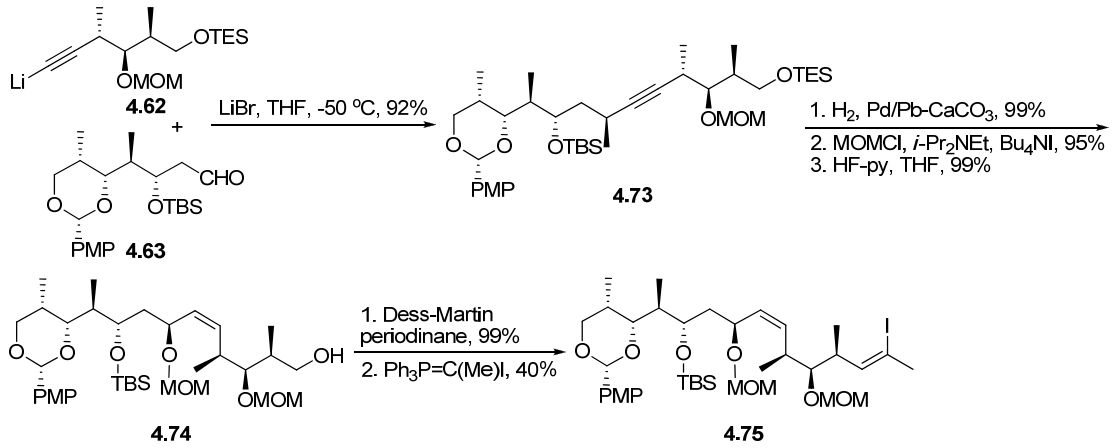

Scheme 4.22 Synthesis of intermediate **4.75**

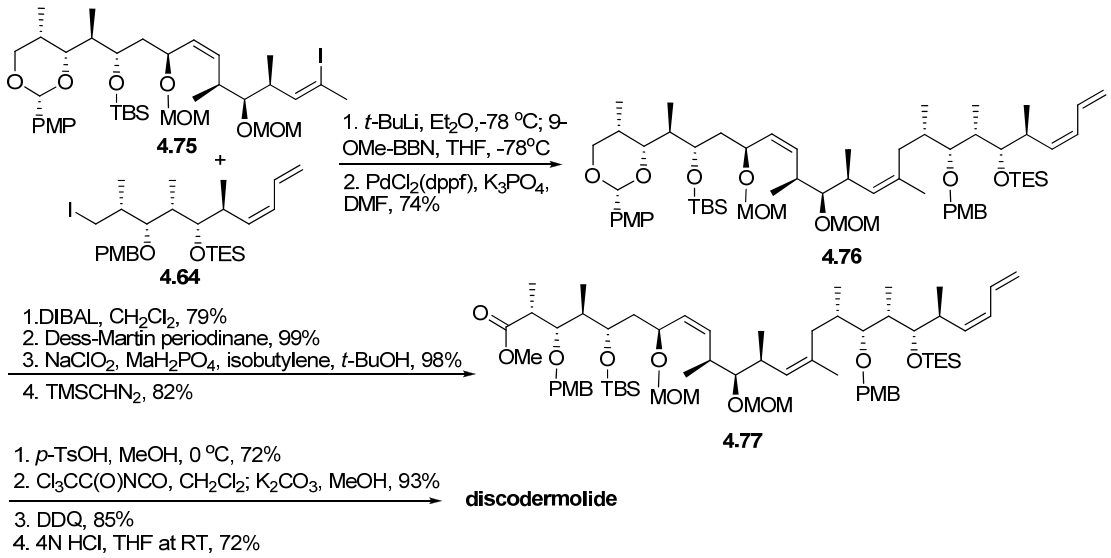

Scheme 4.23 Synthesis of discodermolide

4.4.5 The Paterson Synthesis[39,60-62]

Paterson and co-workers reported their first generation synthesis of discodermolide in 2001, and the retrosynthesis is shown above. In 2003 and 2005, they revised their synthetic approach and published second and third generation syntheses, which overcame the issues of the low yield and poor stereochemistry selectivity in the first generation.

In the first generation of Paterson's strategy, two building blocks **4.78** (Scheme 4.25), **4.79** (Scheme 4.26) were both prepared from a commercially available material **4.81**, and **4.80** was obtained from starting material **4.82** (Scheme 4.27).

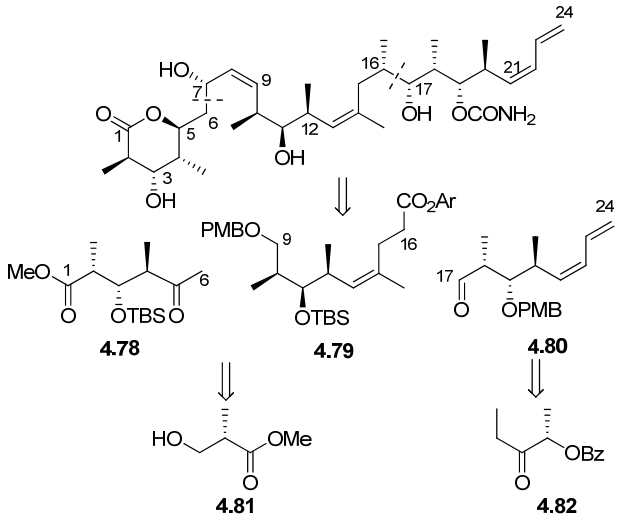

Scheme 4.24 Paterson's retrosynthetic appoach of the first generation

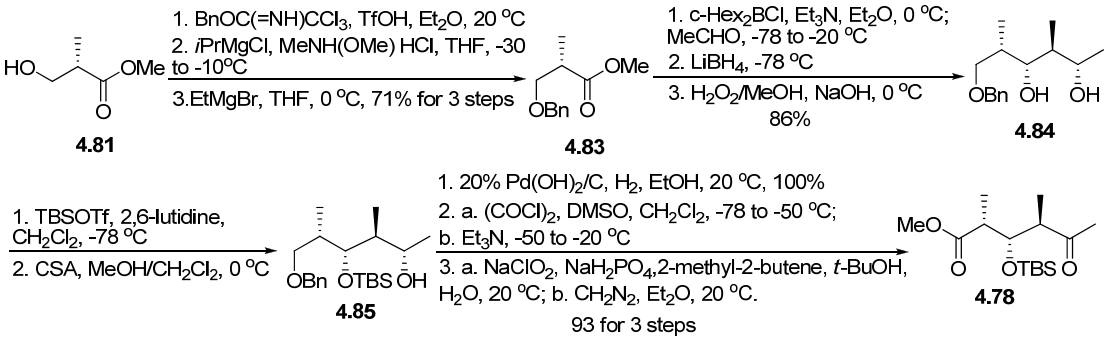

Scheme 4.25 synthesis of subunit **4.78**

The connection of **4.79** to **4.80** was accomplished via aldol reaction and the subsequent manipulations provided **4.93**, which was then coupled with **4.78** via boron-mediated aldol reaction to give methyl ester **4.94**. The following cyclization and global deprotection of silyl protecting groups finally furnished discodermolide in 84% yield (Scheme 4.28).

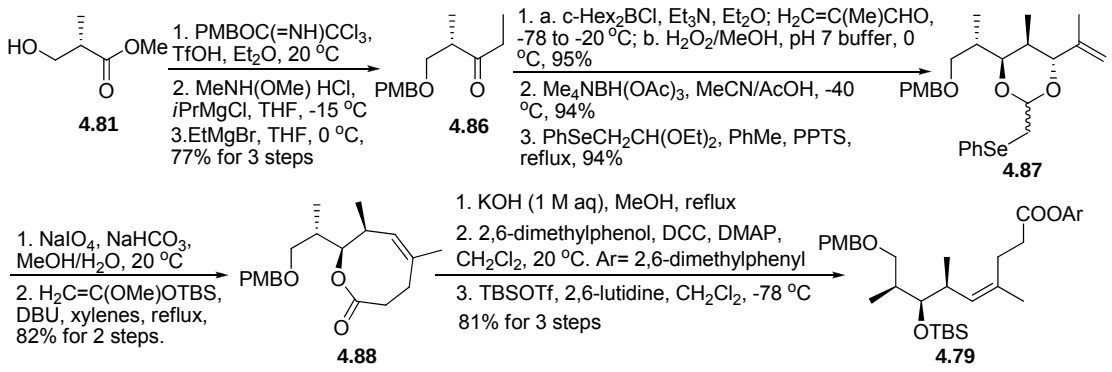

Scheme 4.26 synthesis of subunit **4.79**

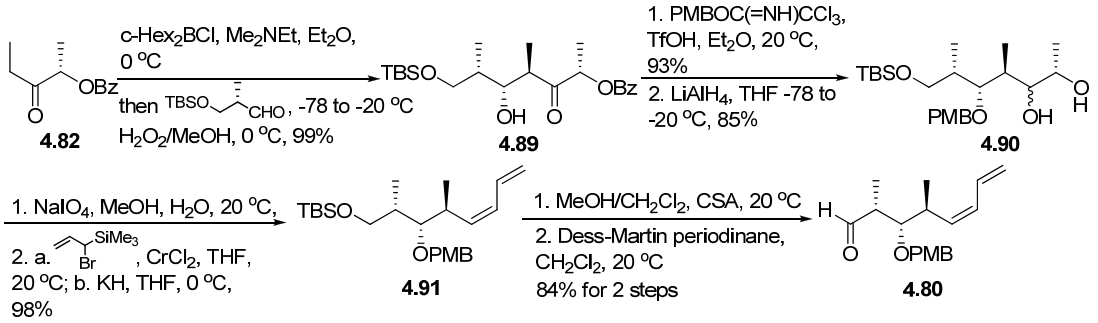

Scheme 4.27 synthesis of subunit **4.80**

The overall yield of the first generation Paterson synthesis was 7.7% through 27 steps, which was improved in comparison with the Schreiber (4.3%), Myles (1.5%), Marshall (1.2%) and Smith syntheses (6%). It was also amenable to the preparation of multi-gram quantities, and this flexible strategy provided a number of diastereomers and structural analogues of discodermolide for further studies on the structure-activity relationships of discodermolide.

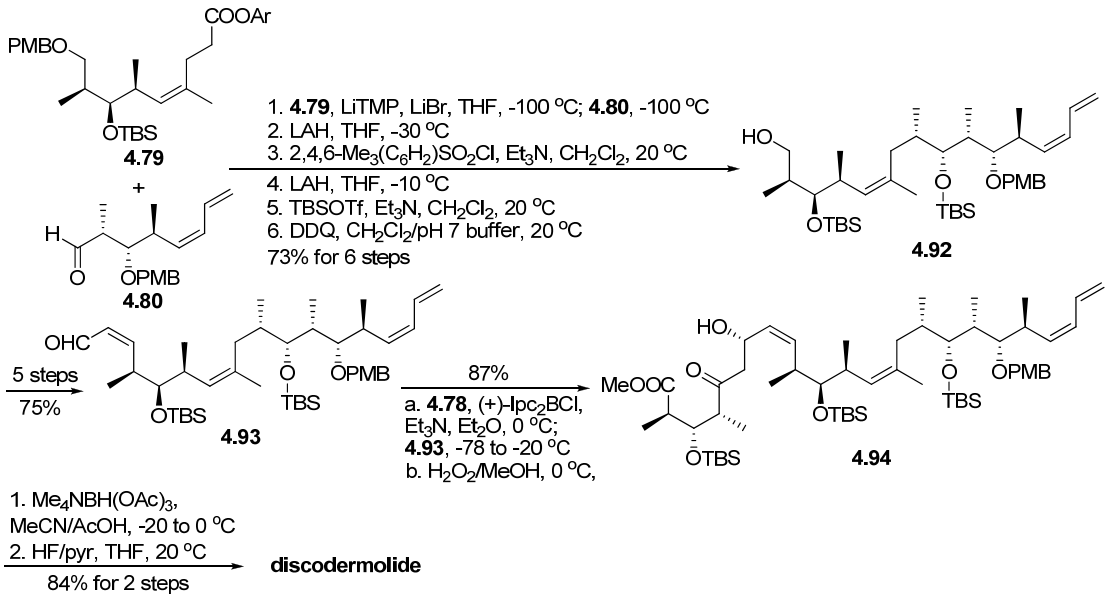

Scheme 4.28 synthesis of discodermolide

4.5 Summary

Since Gunasekera's group first reported the discovery of discodermolide in 1990, this natural product has given people many surprises. This amazing compound was proved to inhibit cell proliferation by inducing cell cycle arrest in the G2/M phase, mitotic bundling and affecting microtubule assembly *in vivo* more rapily than taxol. Of the particular interest is that discodermolide displays potent activity against multi-drug-resistant cancer cell lines. Recently, it has been shown to act synergistically with taxol. These unique properties have already made discodermolide a highly promising candidate as a new chemotherapeutic agent for the treatment of cancer. In 2004, discodermolide entered into

clinical trials as an anticancer agent. Unfortunately, it failed the phase I clinical trials due to its pulmonary toxicity,[72,73] which may hamper its clinical development. The current progress in the total synthesis of discodermolide has alleviated the supply problem and permitted further *in vivo* analysis of its exciting synergism.

References

1. Gunasekera, S. P.; Gunasekera, M.; Longley, R. E., Discodermolide: a new bioactive polyhydroxylated lactone from the marine sponge *Discodermia dissolute*. *J. Org. Chem.* **1990**, *55*, 4912-4915.
2. Kato, Y.; Fusetani, N.; Matsunaga, S.; Hashimoto, K., Bioactive marine metabolites. Part 16. Calyculin A. A novel antitumor metabolite from the marine sponge *Discodermia calyx*. *J. Am. Chem. Soc.* **1986**, *108*, 2780-2781.
3. Kato, Y.; Fusetani, N.; Matsunaga, S.; Hashimoto, K.; Koseki, K. J., Bioactive marine metabolites. 24. Isolation and structure elucidation of calyculins B, C, and D, novel antitumor metabolites, from the marine sponge *Discodermia calyx*. *J. Org. Chem.* **1988**, *53*, 3930-3932.
4. Matsunaga, S.; Fusetani, N.; Konosu, S., Bioactive marine metabolites VI. Structure elucidation of discodermin A, an antimicrobial peptide from the marine sponge *Discodermia kiiensis*. *Tetrahedron Lett.* **1984**, *25*, 5165-5168.

5. Nerenberg, J. B.; Hung, D. T.; Somers, P. K.; Schreiber, S. L., Total synthesis of the immunosuppressive agent (-)-discodermolide. *J. Am. Chem. Soc.* **1993**, *115*, 12621-12622.

6. Smith, III A. B.; Lamarche, M. J.; Falcone-Hindley, M., Solution structure of (+)-discodermolide. *Org. Lett.* **2001**, *3*, 695-698.

7. Monteagudo, E.; Cicero, D. O.; Cornett, B.; Myles, D. C.; Snyder, J. P., The conformations of discodermolide in DMSO. *J. Am. Chem. Soc.* **2001**, *123*, 6929-6930.

8. Hung, D. T.; Nerenberg, J. B.; Schreiber, S. L., Distinct binding and cellular properties of synthetic (+)- and (-)-discodermolides. *Chem. Biol.* **1994**, *1*, 67-71.

9. Hung, D. T.; Nerenberg, J. B.; Schreiber, S. L., Syntheses of discodermolides useful for investigating microtubule binding and stabilization. *J. Am. Chem. Soc.* **1996**, *118*, 11054-11080.

10. Hung, D. T.; Chen, J.; Schreiber, S. L., (+)-Discodermolide binds to microtubules in stoichiometric ratio to tubulin dimmers, blocks taxol binding and results in mitotic arrest. *Chem. Biol.* **1996**, *3*, 287-293.

11. ter Haar, E.; Kowalski, R. J.; Hamel, E.; Lin, C. M.; Longley, R. E.; Gunasekera, S. P.,; Rosenkranz, H. S.; Day, B. W., Discodermolide, a cytotoxic marine agent that stabilizes microtubules more potently than taxol. *Biochem.* **1996**, *35*, 243-250.

12. Kowalski, R. J.; Giannakakou, P.; Gunasekera, S. P.; Longley, R. E.; Day, B. W.;

Hamel, E., The microtubule-stabilizing agent dicodermolide competitively inhibits the binding of paclitaxel (taxol) to tubulin polymers, enhances tubulin nucleation reactions more potently than paclitaxel, and inhibits the growth of paclitaxel-resistant cells. *Mol. Pharm.* **1997**, *52*, 613-622.

13. Martello, L. A.; McDaid, H. M.; Regl, D. L.; Yang, C. H.; Meng, D.; Pettus, T. R. R.; Kaufman, M. D.; Arimoto, H.; Danishefsky, S. J.; Smith, III A. B.; Horwitz, S. B., Taxol and discodermolide represent a synergistic drug combination in human carcinoma cell lines, *Clin. Cancer Res.* **2000**, *6*, 1978-1987.
14. Longley, R. E.; Caddigan, D.; Harmody, D.; Gunasekera, M.; Gunasekera, S. P., Discodermolide- a new, marine-derived immunosuppressive compound. I. in vitro studies. *Transplantation* **1991**, *52*, 650-656.
15. Longley, R. E.; Caddigan, D.; Harmody, D.; Gunasekera, M.; Gunasekera, S. P., Discodermolide: a new, marine-derived immunosuppressive compound. II. *in vivo* studies. *Transplantation* **1991**, *52*, 656-661.
16. Givan, A. L., *In Flow Cytometry First Principles*. Wiley-Liss: New York, 1992; p 110-117.
17. Shapiro, H. P., *In Practical Flow Cytometry*. Alan R. Liss: New York, 1985; p 114-121.
18. Murray, A. W.; Kirschner, M. W., Cyclin synthesis drives the early embryonic cell cycle. *Nature* **1989**, *339*, 275-280.

19. Hurray, A. W.; Solomon, M.; Kirschner, M. W., The role of cyclin synthesis and degradation in the control of maturation promoting factor activity. *Nature* **1989**, *339*, 280-286.

20. Murray, A. W.; Kirschner, M. W., Dominoes and clocks: the union of two views of the cell cycle. *Science* **1989**, *246*, 614-621.

21. Holloway, S. L.; Glotzer, M.; King, R. W.; Murray, A. W., Anaphase is initiated by proteolysis rather than by the inactivation of maturation-promoting factor. *Cell* **1993**, *75*, 1393-1402.

22. Nurse, P., Universal control mechanism regulating onset of M-phase. *Nature* **1990**, *344*, 503-508.

23. Murray, A.; Hunt, T., *The Cell Cycle*. W. H. Freeman: New York, 1993.

24. Rieder, C. L., Colcemid and the mitotic cycle. *J. Cell Sci.* **1992**, *102*, 387-392.

25. Schiff, P. B.; Horwitz S. B., Taxol stabilizes microtubules in mouse fibroblast cells. *Proc. Natl. Acad. Sci.* **1980**, *77*, 1561-1565.

26. Kumar, N., Taxol-induced polymerization of purified tubulin. *J. Biol. Chem.* **1981**, *256*, 10435-10441.

27. Parness, J.; Horwitz, S. B., Taxol binds to polymerized tubulin *in vitro*. *J. Cell Biol.* **1981**, *91*, 479-487.

28. Martello, L. A.; Lamarche, M. J.; He, L.; Beauchamp, T. J.; Smith, III A. B.; Horwitz, S. B., The relationship between taxol and (+)-discodermolide: synthetic

analogs and modeling studies. *Chem. Biol.* **2001**, *8*, 843-855.

29. Burlingame, M. A.; Shaw, S. J.; Sundermann, K. F.; Zhang, D.; Petryka, J.; Mendoza, E.; Liu, F.; Myles, D. C.; LamMarche, M. J.; Hirose, T.; Freeze, B. S.; Smith, III A. B., Design, synthesis and cytotoxicity of 7-deoxy aryl discodermolide analogues. *Bioorg. Med. Chem. Lett.* **2004**, *12*, 2335-2338.

30. Honore, S.; Kamath, K.; Braguer, D.; Horwitz, S. B.; Wilson, L.; Briand, C.; Jordan, M. A., Synergistic suppression of microtubule dynamics by discodermolide and paclitaxel in non-small cell lung carcinoma cells. *Cancer Res.* **2004**, *64*, 4957-4964.

31. Gunasekera, S. P.; Longley, R. E.; Isbrucker, R. A., Semisynthetic analogues of the microtubule-stabilizing agent discodermolide: preparation and biological activity. *J. Nat. Prod.* **2002**, *65*, 1830-1837.

32. Gunasekera, S. P.; Mickel, S. J.; Daeffler, R.; Niederer, D.; Wright, A. E.; Linley, P.; Pitts, T., Synthetic analogues of the microtubule-stabilizing agent (+)-discodermolide: preparation and biological activity. *J. Nat. Prod.* **2004**, *67*, 749-756.

33. Roush, W. R.; Palkowitz, A. D.; Ando, K., Acyclic diastereoselective synthesis using tartrate ester-modified crotylboronates. Double asymmetric reactions with α-methyl chiral aldehydes and synthesis of the C(19)-C(29) segment of rifamycin S. *J. Am. Chem. Soc.* **1990**, *112*, 6348-6359.

34. Isbrucker, R. A.; Gunasekera, S. P.; Longley, R. E., Stucture-activity relationship

studies of discodermolide and its semisynthetic acetylated analogs on microtubule function and cytotoxicity. *Cancer Chemother. Pharmacol.* **2001**, *48*, 29-36.

35. Gunasekera, S. P.; Longley, R. E.; Isbrucker, R. A., Acetylated analogues of the microtubule-stabilizing agent discodermolide: preparation and biological activity. *J. Nat. Prod.* **2001**, *64*, 171-174.

36. Smith, III, A. B.; Freeze, B. S.; LaMarche, M. J.; Sager, J.; Kinzler, K. W.; Vogelstein, B., Discodermolide analogues as the chemical component of combination bacteriolytic therapy. *Bioorg. Med. Chem. Lett.* **2005,** *15*, 3623-3626.

37. Smith, A. B. III; Freeze, B. S.; Lamarche, M. J.; Hirose, T.; Brouard, I.; Rucker, P. V.; Xian, M.; Sundermann, K. F.; Shaw, S. J.; Burlingame, M. A.; Horwitz, S. B.; Myles, D. C., Design, synthesis, and evaluation of carbamate-substituted analogues of (+)-discodermolide. *Org. Lett.* **2005,** *7*, 311-314.

38. Mınguez, J. M.; Kim, S.-Y.; Giuliano, K. A.; Balachandran, R.; Madiraju, C.; Day, B. W.; Curran, D. P., Synthesis and biological assessment of simplified analogues of the potent microtubule stabilizer (+)-discodermolide. *Bioorg. Med. Chem.* **2003,** *11*, 3335-3357.

39. Paterson, I.; Florence, G. J.; Gerlach, K.; Scott, J. P.; Sereinig, N., A practical synthesis of (+)-discodermolide and analogues: fragment union by complex aldol reactions. *J. Am. Chem. Soc.* **2001**, *123*, 9535-9544.

40. Myles, D. C., Novel biologically active natural and unnatural products. *Curr. Opin.*

Biotechnol. **2003**, *14*, 627-633.

41. Clark, D. L.; Heathcock, C. H., Studies on the alkylation of chiral enolates: application toward the total synthesis of discodermolide. *J. Org. Chem.* **1993**, *58*, 5878-5879.

42. Paterson, I.; Wren, S. P., Studies towards the total synthesis of the marine-derived immunosuppressant discodermolide; asymmetric synthesis of a C1–C8 δ-lactone subunit. *J. Chem. Soc. Chem. Commun.* **1993**, 1790-1792.

43. Golec, J. M. C.; Jones, S. D., The synthesis of a C1-C8 lactone fragment of discodermolide. *Tetrahedron Lett.* **1993**, *34*, 8159-8162.

44. Evans, P. L.; Golec, J. M. C.; Gillespie, R. J., The synthesis of a C9-C17, fragment of discodermolide. *Tetrahedron Lett.* **1993**, *34*, 8163-8166.

45. Golec, J. M. C.; Gillespie, R. J., An approach to the synthesis of a C9-C15 fragment of discodermolide. *Tetrahedron Lett.* **1993**, *34*, 8167-8168.

46. Miyazawa, M.; Mitsuoka, E.; Sasaki, S.; Oonuma, S.; Maruyama, K.; Miyashita, M., Expeditious and stereoselective synthesis of chiral trans-β-hydroxy-δ-lactone systems. *Chem. Lett.* **1998**, *27*, 109-110.

47. Evans, D. A.; Halstead, D. P.; Allison, B. D., Chelation-controlled stannylacetylene additions to β-alkoxy aldehydes promoted by alkylaluminum halide Lewis acids. *Tetrahydron Lett.* **1999**, *40*, 4461-4462.

48. Filla, S. A.; Song, J. J.; Chen, L.; Masamune, S., Synthesis of C1-C8 and C9-C24

fragments of (−)-discodermolide: use of asymmetric alkylation and stereoselective aldol reactions. *Tetrahedron Lett.* **1999**, *40*, 5449-5453.

49. Misske, A. M.; Hoffmann, H. M. R., Asymmetric synthesis of seven-carbon segments of the phorboxazoles and (−)-discodermolide: Complementary route from racemic *trans*-2,4-dimethyl-8-oxabicyclo[3.2.1]oct-6-en-3-one. *Tetrahedron* **1999**, *55*, 4315-4324.

50. Yang, G.; Myles, D.C., An alkylative strategy to the C-13 to C-21 sector of discodermolide. *Tetrahedron Lett.* **1994**, *35*, 1313-1316.

51. Yang, G.; Myles D.C., The synthesis of the C-9 to C-21 sector of discodermolide: An efficient route to the C13–14 *Z*-trisubstituted alkene. *Tetrahedron Lett.* **1994**, *35*, 2503-2504.

52. Harrid, S. S.; Yang, G.; Strawn, M. A.; Myles, D. C., Total synthesis of (-)-discodermolide: an application of a chelation-controlled alkylation reaction. *J. Org. Chem.* **1997**, *62*, 6098-6099.

53. Francavilla, C.; Chen, W.; Kinder, Jr. F. R., Formal synthesis of (+)-discodermolide. *Org. Lett.* **2003**, *5*, 1233-1236.

54. Sill, W. C.; Gennari, C., Direct synthesis of *Z*-unsaturated esters. A useful modification of the Horner-Emmons olefination. *Tetrahedron Lett.* **1983**, 24, 4405-4408.

55. Rychnovsky, S. D.; Togers, B.; Yang, G., Analysis of two carbon-13 NMR

correlations for determining the stereochemistry of 1,3-diol acetonides. *J. Org. Chem.* **1993**, *58*, 3511-3515.

56. Harried, S. S.; Lee, C. P.; Yang, G.; Lee, T. I. H.; Myles, D. C., Total synthesis of the potent microtubule stabilizing agent (+)-discodermolide. *J. Org. Chem.* **2003**, *68*, 6646-6660.

57. Mori, Y.; Kuhara, M.; Takeuchi, A.; Suzuki, M., Stereoselective reduction of β-alkoxy ketones: a synthesis of syn-1,3-diols, *Tetrahedron Lett.* **1988**, 29, 5419-5422.

58. Marshall, J. A.; Johns, B. A., Total synthesis of (+)-discodermolide. *J. Org. Chem.* **1998**, *63*, 7885-7892.

59. Paterson, I.; Florence, G. J.; Gerlach, K.; Scott, J. P.; Sereinig, N., A practical synthesis of (+)-discodermolide and analogues: fragment union by complex aldol reactions. *J. Am. Chem. Soc.* **2001**, *123*, 9535-9544.

60. Paterson, I.; Delagdo, O.; Florence, G. J.; Lyothier, I.; Scott, J. P.; Sereinig, N., 1,6-Asymmetric induction in boron-mediated aldol reactions: application to a practical total Synthesis of (+)-discodermolide. *Org. Lett.* **2003**, *5*, 35-38.

61. Paterson, I.; Florence, G. J.; Gerlach, K.; Scott, J. P., Total synthesis of the antimicrotubule agent (+)-discodermolide using boron-mediated aldol reactions of chiral ketones. *Angew. Chem., Int. Ed.* **2000**, *39*, 377-380.

62. Paterson, I.; Florence, G. J., Synthesis of (+)-discodermolide and analogues by

control of asymmetric induction in aldol reactions of λ-chiral (*Z*)-enals. *Tetrahedron Lett.* **2000**, *41*, 6935-6939.

63. Smith, III A. B.; Qiu, Y.; Jones, D. R.; Kobayashi, K., Total synthesis of (-)-discodermolide. *J. Am. Chem. Soc.* **1995**, *117*, 12011-12012.

64. Smith, III A. B.; Kaufman, M. D.; Beauchamp, T. J.; Lamarche, M. J.; Arimoto, H., Gram-scale synthesis of (+)-discodermolide. *Org. Lett.* **1999**, *1*, 1823-1826.

65. Smith, III A. B.; Freeze, B. S.; Brouard, I.; Tomoyasu, H., A practical improvement, enhancing the large-scale synthesis of (+)-discodermolide: a third-generation approach. *Org. Lett.* **2003**, *5*, 4405-4408.

66. Smith, III A. B.; Beauchamp, T. J.; LaMarche, M. J.; Kaufman, M. D.; Qiu, Y.; Arimoto, H.; Jones, D. R; Kobayashi, K., Evolution of a gram-scale synthesis of (+)-discodermolide. *J. Am. Chem. Soc.* **2000**, *122*, 8654-8664.

67. Negishi, E.; Valente, L. F.; Kobayashi, M., Palladium-catalyzed cross-coupling reaction of homoallylic or homopropargylic organozincs with alkenyl halides as a new selective route to 1,5-dienes and 1,5-enynes. *J. Am. Chem. Soc.* **1980**, *102*, 3298-3299.

68. Koěovský, P., Carbamates: A method of synthesis and some syntehtic applications. *Tetrahedron Lett.* **1986**, *27*, 5521-5524.

69. Mínguez, J. M.; Kim, S.; Giuliano, K. A.; Balachandran, R.; Madiraju, C.; Day, B. W.,; Curran, D. P., Synthesis and biological assessment of simplified analogues of

the potent microtubule stabilizer (+)-discodermolide. *Bioorg. Med. Chem.* **2003**, *11*, 3335-3357.

70. Kalesse, M., The chemistry and biology of discodermolide. *Chem. Biochem.* **2000**, *1*, 171-175.

71. Nagaoka, H.; Kishi, Y., Further synthetic studies on rifamycins. *Tetrahedron* **1981**, *37*, 3873-3888.

72. Mita, A.; Lockhart, A. C.; Chen, T.-L.; Bochinski, K.; Curtright, J.; Cooper, W.; Hammond, L.; Rothenberg, M.; Rowinsky, E.; Sharma, S., A phase I pharmacokinetic (PK) trial of XAA296A (discodermolide) administered every 3 weeks to adult patients with advanced solid malignancies. *Proc. Am. Soc. Clin. Oncol.* **2004**, *22*, 2025.

73. Attard, G.; Greystoke, A.; Kaye S.; De Bono, J., Update on tubulin-binding agents. *Pathol. Biol.* **2006**, *54*, 72-84.